

ESR Characterization of Hexameric, Helical Peptides Using Double TOAC Spin Labeling

Paul Hanson,[†] Glenn Millhauser,^{*,†} Fernando Formaggio,[‡] Marco Crisma,[‡] and Claudio Toniolo[‡]

Contribution from the Department of Chemistry and Biochemistry, University of California at Santa Cruz, Santa Cruz, California 95064, and Biopolymer Research Center, CNR, Department of Organic Chemistry, University of Padova, 35131 Padova, Italy

Received March 28, 1996[⊗]

Abstract: α -Aminoisobutyric acid (Aib) is a C $^{\alpha}$ -tetrasubstituted amino acid that strongly favors helical structure. Most of the conformational trends established for Aib-rich peptides have been determined by X-ray crystallography. Whether these conformational trends carry over to protic solvents is an open question. In order to develop a general strategy for probing the properties of peptides containing C $^{\alpha}$ -tetrasubstituted amino acids, the hexameric sequences Boc-TOAC-Ala $_n$ -TOAC-Ala $_{4-n}$ -OtBu were synthesized where $n = 0-3$ and TOAC is a spin label Aib analog. The peptides were studied by electron spin resonance (ESR) in four alcohols: MeOH, EtOH, TFE, and HFIP. Biradical J -coupling and dipolar interactions between the TOACs within each peptide were used to determine peptide geometry as a function of solvent. In MeOH, strong biradical interactions were observed consistent with the geometry of a 3_{10} -helix. The solvents displayed differing tendencies to support helical structure with the ranking MeOH > EtOH > TFE > HFIP. In HFIP, there were no indications of residual helical structure. While C $^{\alpha}$ -tetrasubstituted amino acids do favor the helix, these data demonstrate that such amino acids do not “lock in” the helical conformation. Qualitative analysis of the line width variations for the hexamers in MeOH suggests that the interconversion time for helix \rightarrow coil is several nanoseconds. Additional peptides were prepared in order to explore the effects of peptide length, N-terminal blocking group, and insertion of an additional Aib.

Introduction

The stability and folding of helical regions in proteins and natural peptides are often investigated using designed helical peptides as models. Several useful techniques are available to characterize peptide helices. The most widely used are X-ray crystallography, nuclear magnetic resonance (NMR) and circular dichroism (CD) spectroscopy. For solution work, NMR yields local folding information while CD provides a global view of helical content. Each spectroscopic technique provides a unique but incomplete picture of the peptide conformers. To resolve further the many structural issues that arise in the study of helical peptides, we have explored the use of double label electron spin resonance (ESR).¹⁻⁴ Two nitroxide spin labels are covalently attached to amino acid side chains and the labels interact over distances that are typically longer than sampled by nuclear Overhauser enhancement (NOE) NMR spectroscopy. Thus, double label ESR provides a unique and often complementary view of the local peptide structure. For example, there are two common helical structures: α -helices ($i \leftarrow i + 4$ hydrogen bonding) and 3_{10} -helices ($i \leftarrow i + 3$ hydrogen bonding). Distinguishing helical conformations using NMR or CD can be difficult, especially when studying short linear peptides. However, double label ESR performed on a series of peptides suggests that 16-residue Ala-rich sequences⁵ contain a mixture

of the two helical conformers and the relative populations depend on peptide length and sequence.^{1,3,4} This finding is supported by recent theoretical calculations and has resulted in a reevaluation of the statistical mechanical helix-coil theory.⁶ Further, double label ESR is now being used in the determination of quantitative distances in immobile peptides.⁷

α -Aminoisobutyric acid (Aib) is a strong helix-favoring amino acid.⁸⁻¹¹ It is achiral, tetrasubstituted at the α -carbon, and a common component of a class of microbial peptides. Because Aib is more helix favoring than any of the protein amino acids, it has received increasing attention in the field of peptide design. To date, most of the detailed structural information on Aib-rich peptides has come from crystallographic studies.¹⁰⁻¹⁵ Such studies have revealed a wealth of information including the effect of length and Aib content on the 3_{10} -helix \rightarrow α -helix equilibrium and structural heterogeneity within a helix. Unfortunately, the number of structural studies on Aib-rich peptides in solution is much more limited. Pioneering NMR and infrared experiments performed by Scheraga and co-workers demonstrated the tendency of short (Aib) $_n$ peptides to form 3_{10} -helices

(6) Sheinerman, F. B.; Brooks, C. L. *J. Am. Chem. Soc.* **1995**, *117*, 10098–10103.

(7) Rabenstein, M. D.; Shin, Y.-K. *Proc. Natl. Acad. Sci. U.S.A.* **1995**, *92*, 8239–8243.

(8) Paterson, Y.; Rumsey, S. M.; Benedetti, E.; Nemethy, G.; Scheraga, H. A. *J. Am. Chem. Soc.* **1981**, *103*, 2947–2955.

(9) Marshall, G. R. In *Intra-Science Chemistry Reports*; Kharasch, N., Ed.; Gordon and Breach: New York, 1971; Vol. 5, pp 305–316.

(10) Karle, I. L.; Balam, P. *Biochemistry* **1990**, *29*, 6747–6756.

(11) Toniolo, C.; Benedetti, E. *Macromolecules* **1991**, *24*, 4004–4009.

(12) Karle, I. L.; Flippen-Anderson, J. L.; Uma, K.; Balam, P. *Biopolymers* **1993**, *33*, 827–837.

(13) Karle, I. L.; Flippen-Anderson, J. L.; Uma, K.; Balam, P. *Int. J. Pept. Protein Res.* **1994**, *44*, 491–498.

(14) Karle, I. L.; Flippen-Anderson, J.; Gurunath, R.; Balam, P. *Protein Sci.* **1994**, *3*, 1547–1555.

(15) Karle, I. L. *Biopolymers* **1996**, *40*, 157–180.

[†] University of California at Santa Cruz.

[‡] University of Padova.

[⊗] Abstract published in *Advance ACS Abstracts*, August 1, 1996.

(1) Millhauser, G. L. *Biochemistry* **1995**, *34*, 3873–3877, 10318.

(2) Miick, S. M.; Martinez, G. V.; Fiori, W. R.; Todd, A. P.; Millhauser, G. L. *Nature* **1992**, *359*, 653–655; and **1995**, *377*, 257.

(3) Fiori, W. R.; Lundberg, K. M.; Millhauser, G. L. *Nature: Struct. Biol.* **1994**, *1*, 374–377.

(4) Fiori, W. F.; Miick, S. M.; Millhauser, G. L. *Biochemistry* **1993**, *32*, 11957–11962.

(5) Marqusee, S.; Robbins, V. H.; Baldwin, R. L. *Proc. Natl. Acad. Sci. U.S.A.* **1989**, *86*, 5286–5290.

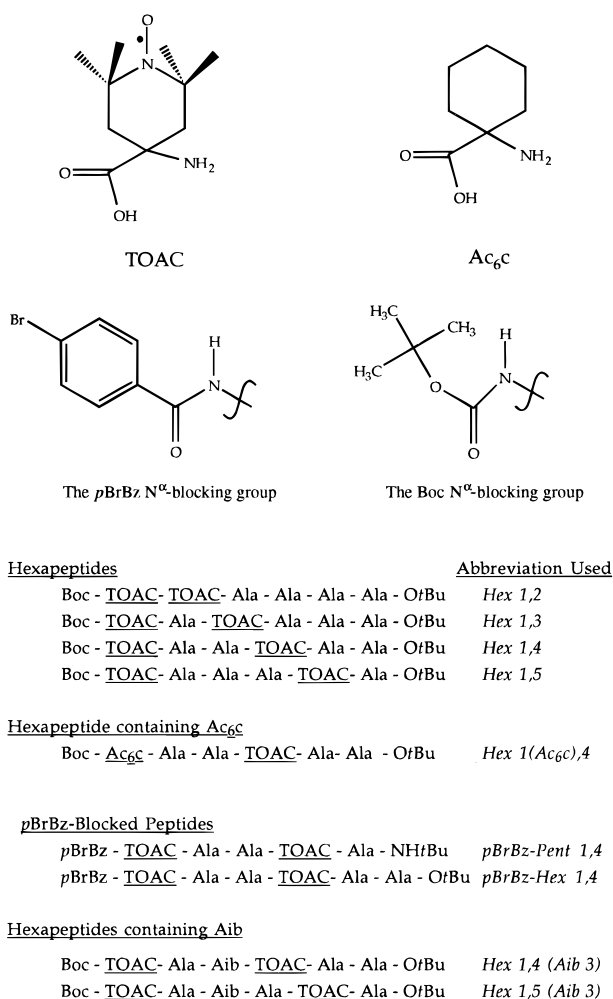


Figure 1. Structure of TOAC, the TOAC analog 1-aminocyclohexanecarboxylic acid (Ac₆C), the N-terminal blocking groups, and the hexapeptides examined in this study.

in various solvents.¹⁶ Kuki and colleagues have made important contributions using NMR spectroscopy to examine Aib-rich peptides in polar, aprotic solvents.^{17–21} However, NOE studies are hampered by the lack of a C^α proton in Aib and the short correlation time of small peptides.

The use of the novel, unnatural α -amino acid 2,2,6,6-tetramethylpiperidine-1-oxyl-4-amino-4-carboxylic acid (TOAC; see Figure 1) is explored here in a structural study of hexameric sequences. Incorporation of TOAC into peptide sequences serves two purposes. First, TOAC is tetrasubstituted at the α -carbon and thus possesses the strong helix-promoting characteristics of Aib. Second, TOAC is a nitroxide and serves as a rigidly-attached spin label at any chosen position. The TOAC label was first synthesized nearly three decades ago²² and introduced into the realm of peptide chemistry within the last fifteen years.²³ In recently published work, double TOAC labeling has proven to be remarkably sensitive to peptide geometry.^{24–26}

(16) Paterson, Y.; Stimson, E. R.; Evans, D. J.; Leach, S. J.; Scheraga, H. A. *Int. J. Pept. Protein Res.* **1982**, *20*, 468–480.

(17) Augspurger, J. D.; Bindra, V. A.; Scheraga, H. A.; Kuki, A. *Biochemistry* **1995**, *34*, 2566–2576.

(18) Bindra, V. A.; Kuki, A. *Int. J. Pept. Protein Res.* **1994**, *44*, 539–548.

(19) Basu, G.; Kuki, A. *Biopolymers* **1993**, *33*, 995–1000.

(20) Basu, G.; Kuki, A. *Biopolymers* **1992**, *32*, 61–71.

(21) Basu, G.; Bagchi, K.; Kuki, A. *Biopolymers* **1991**, *31*, 1763–1774.

(22) Rassat, A.; Rey, P. *Bull. Chem. Soc. Fr.* **1967**, 815–817.

(23) Nakaie, C. L.; Goissis, G.; Schreier, S.; Paiva, A. C. M. *Braz. J. Med. Biol. Res.* **1981**, *14*, 173–180.

The conformation of Ala-based hexameric sequences was examined here with a double TOAC labeling strategy. Hexamers were chosen as they are sufficiently long so that, with the assistance of the TOACs, they are expected to form stable 3₁₀-helices.^{10,11} This length should not, however, appreciably favor α -helix over 3₁₀-helix. Short Ala-rich peptides are marginally stable in the helical conformation (see recent discussions on the helix-promoting character of Ala^{27–31}) and thus are quite sensitive to many factors (*i.e.*, length, sequence, and solvent) which control helical content in peptides. The sequences examined are shown in Figure 1. Three sets of peptides were synthesized to explore the influences of solvent, length, N-terminal blocking group, and Aib insertion on helical structure. In the first set, placement of the labels $i \rightarrow i + 1$ through $i \rightarrow i + 4$ (*Hex-1,2* through *Hex-1,5*) provides a probe of the type of helical turn adopted by a hexapeptide. In the second set, a pentapeptide (*p*BrBz-*Pent-1,4*, where *p*BrBz is *p*-bromobenzoyl)²⁴ is compared to a hexapeptide (*p*BrBz-*Hex-1,4*) in order to probe the effects of main chain length. In addition, comparison of *p*BrBz-*Hex-1,4* with *Hex-1,4* determines whether the conjugated *p*BrBz N-terminal blocking group stabilizes the helix. The final set of peptides contains an Aib between the labels (*Hex-1,4* (Aib 3) and *Hex-1,5* (Aib 3)). This latter set probes the tendency of Aib to confer additional stability on helical structure. Each of the peptides was examined in four neat alcohols which promote helical structure to varying degrees. This strategy allows the determination of each peptide's resistance to unfolding. Furthermore, ranking the helix-promoting characteristics of each solvent enables comparison of our experimental results with both recent molecular dynamics calculations and crystallographic studies.

Materials and Methods

Synthesis and Characterization of Peptides. Melting points were determined using a Leitz (Wetzlar, Germany) model Laborlux 12 apparatus and are not corrected. Optical rotations were measured using a Perkin-Elmer (Norwalk, CT) model 241 polarimeter equipped with a Haake (Karlsruhe, Germany) model D thermostat. Thin-layer chromatography was performed on Merck (Darmstadt, Germany) Kieselgel 60F₂₅₄ precoated plates using the following solvent systems: 1 (CHCl₃-EtOH, 9:1); 2 (BuⁿOH-AcOH-H₂O, 3:1:1); 3 (toluene-EtOH, 7:1). The chromatograms were examined by using UV fluorescence or developed by chlorine-starch-potassium iodide or ninhydrin chromatic reaction as appropriate. All the compounds were obtained in a chromatographically homogeneous state. Amino acid analysis of the Ala/TOAC peptides was not performed as TOAC is unstable under the acidic conditions required for the hydrolysis of the -CONH-, -OCONH-, and -COO- bonds.

The free amino acid TOAC and its Fmoc and Boc N^α-protected derivatives were prepared according to published procedures.²⁴ Since the acidic and reducing conditions required to remove the Boc and Z groups, respectively, are not compatible with the full chemical integrity

(24) Toniolo, C.; Valente, E.; Formaggio, M.; Crisma, G.; Pilloni, G.; Corvaja, C.; Toffoletti, A.; Martinez, G. V.; Hanson, M. P.; Millhauser, G. L.; George, C.; Flippen-Anderson, J. L. *J. Pept. Sci.* **1995**, *1*, 45–57.

(25) Hanson, P.; Martinez, G.; Millhauser, G.; Formaggio, F.; Crisma, M.; Toniolo, C.; Vita, C. *J. Am. Chem. Soc.* **1996**, *118*, 271–272.

(26) Smythe, M. L.; Nakaie, C. R.; Marshall, G. R. *J. Am. Chem. Soc.* **1995**, *117*, 10555–10562.

(27) Vila, J.; Williams, R. L.; Grant, J. A.; Wojcik, J.; Scheraga, H. A. *Proc. Natl. Acad. Sci. U.S.A.* **1992**, *89*, 7821–7825.

(28) Chakrabarty, A.; Schellman, J. A.; Baldwin, R. L. *Nature* **1991**, *351*, 586–588.

(29) Chakrabarty, A.; Kortemme, T.; Baldwin, R. L. *Protein Sci.* **1994**, *3*, 843–852.

(30) Kemp, D. S.; Boyd, J. G.; Muendel, C. C. *Nature* **1991**, *352*, 451–454.

(31) Kemp, D. S.; Oslick, S. L.; Allen, T. J. *J. Am. Chem. Soc.* **1996**, *118*, 4249–4255.

(32) Carpino, L. A. *J. Am. Chem. Soc.* **1993**, *115*, 4397–4398.

Table 1. Physical Properties of the TOAC Peptides

compd	melting point (°C)	recryst. solvent ^a	[α] _D ²⁰ (deg) ^b	TLC			vis		IR ^e
				R _{F1}	R _{F2}	R _{F3}	λ _{max}	ε ^d	
Fmoc-TOAC-L-Ala-OrBu	155–156	AcOEt/PE	–15.1	0.95	0.95	0.60	425	7.3	3385, 3321, 1728, 1712, 1660, 1521
Fmoc-L-Ala-TOAC-L-Ala-OrBu	193–194	AcOEt/PE	–61.9	0.95	0.95	0.55	428	7.0	3390, 3310, 1738, 1699, 1680, 1646, 1539
Fmoc-TOAC-(L-Ala) ₂ -OrBu	180–181	AcOEt/PE	–26.6	0.95	0.95	0.50	425	8.3	3392, 3315, 1722, 1714, 1664, 1523
Fmoc-(L-Ala) ₂ -TOAC-L-Ala-OrBu	207–208	AcOEt/PE	–55.5	0.90	0.95	0.45	428	7.4	3421, 3355, 1726, 1691, 1674, 1644, 1532
Fmoc-L-Ala-TOAC-(L-Ala) ₂ -OrBu	141–142	AcOEt/PE	–47.8	0.95	0.95	0.50	428	6.3	3331, 1725, 1675, 1526
Fmoc-TOAC-(L-Ala) ₃ -OrBu	161–163	AcOEt/PE	–21.0	0.70	0.95	0.40	426	5.9	3320, 1722, 1661, 1528
Fmoc-Aib-L-Ala-TOAC-L-Ala-OrBu	163–164	Et ₂ O/PE	–46.1	0.75	0.95	0.40	430	6.6	3360, 1742, 1689, 1661, 1527
Fmoc-Aib-TOAC-(L-Ala) ₂ -OrBu	120–122	AcOEt/PE	–3.5	0.95	0.95	0.50	428	8.8	3335, 1726, 1671, 1521
Fmoc-(L-Ala) ₃ -TOAC-L-Ala-OrBu	213–214	AcOEt/PE	–52.5	0.70	0.95	0.35	424	10.1	3329, 1731, 1700, 1659, 1530
Fmoc-(L-Ala) ₂ -TOAC-(L-Ala) ₂ -OrBu	142–143	CHCl ₃ /PE	–45.2	0.90	0.95	0.40	428	5.9	3334, 1728, 1700, 1664, 1530
Fmoc-L-Ala-TOAC-(L-Ala) ₃ -OrBu	155–157	AcOEt/PE	–30.3	0.70	0.95	0.40	428	5.7	3328, 1726, 1658, 1528
Fmoc-TOAC-(L-Ala) ₄ -OrBu	196–197	AcOEt/PE	–21.4	0.60	0.95	0.35	424	6.4	3343, 3323, 1725, 1698, 1665, 1535
Fmoc-L-Ala-Aib-L-Ala-TOAC-L-Ala-OrBu	141–143	EtOH:Et ₂ O 1:4/PE	–38.3	0.95	0.95	0.40	424	6.1	3329, 1730, 1666, 1531
Fmoc-L-Ala-Aib-TOAC-(L-Ala) ₂ -OrBu	145–146	AcOEt/PE	–19.9	0.95	0.95	0.40	428	6.4	3324, 1724, 1661, 1526
Boc-TOAC-(L-Ala) ₃ -TOAC-L-Ala-OrBu	148–149	AcOEt/PE	2.6	0.65	0.90	0.25	428	13.5	3329, 1727, 1695, 1663, 1528
Boc-TOAC-(L-Ala) ₂ -TOAC-(L-Ala) ₂ -OrBu	135–137	AcOEt/PE	40.3	0.75	0.85	0.20	422	13.0	3324, 1726, 1700, 1660, 1531
Boc-TOAC-L-Ala-TOAC-(L-Ala) ₃ -OrBu	163–164	AcOEt/PE	42.9	0.55	0.90	0.20	420	11.7	3326, 1727, 1661, 1529
Boc-(TOAC) ₂ -(L-Ala) ₄ -OrBu	185–186	AcOEt/PE	39.5	0.70	0.90	0.30	426	10.7	3323, 1726, 1659, 1531
Boc-TOAC-L-Ala-Aib-L-Ala-TOAC-L-Ala-OrBu	227–228	AcOEt/PE	12.9	0.70	0.95	0.25	428	14.5	3332, 1729, 1662, 1531
Boc-TOAC-L-Ala-Aib-TOAC-(L-Ala) ₂ -OrBu	212–213	AcOEt/PE	40.5	0.90	0.90	0.30	425	12.3	3322, 1727, 1663, 1529
Fmoc-TOAC-(L-Ala) ₂ -TOAC-(L-Ala) ₂ -OrBu	163–165	AcOEt/Et ₂ O	8.4	0.80	0.90	0.25	420	11.5	3327, 1729, 1660, 1530
pBrBz-TOAC-(L-Ala) ₂ -TOAC-(L-Ala) ₂ -OrBu	246–247	AcOEt/PE	45.5	0.65	0.85	0.20	420	13.0	3329, 1733, 1660, 1530
Boc-Ac ₆ C-(L-Ala) ₂ -TOAC-(L-Ala) ₂ -OrBu	140–141	AcOEt/PE	18.4	0.60	0.90	0.25	412	8.3	3318, 1728, 1700, 1657, 1529

^a AcOEt, ethyl acetate; PE, petroleum ether; Et₂O, diethyl ether; CHCl₃, chloroform, EtOH, ethyl alcohol. ^b ^c 0.5, methanol. ^c [α]_D²⁰₄₃₆. ^d λ_{max} (nm) and ε (L mol^{–1} cm^{–1}); all vis spectra were recorded in methanol. ^e The solid-state IR spectra were obtained in KBr pellets (only bands in the 3450–3300- and 1800–1500-cm^{–1} regions are reported).

of the nitroxide moiety,²⁴ the Fmoc N^α-protecting group was chosen for the stepwise elongation of TOAC containing peptides. The N-terminal TOAC residue was introduced as the N^α-Boc derivative, with the exception of the pBrBz-TOAC-hexapeptide, where the pBrBz group was introduced through its OBt ester on the N^α-deprotected TOAC hexapeptide.

The Fmoc group was removed by treatment with a 10% diethylamine solution in acetonitrile. After evaporation of the solvent, the NH₂-free peptide was dissolved in chloroform and isolated by elution through a 3 cm bed of silicagel using a chloroform–ethanol 8:2 mixture.

The Ala and Aib residues were incorporated using the symmetrical anhydride approach (method I), while the TOAC residues were introduced by the 1-hydroxybenzotriazole (HOBt)-mediated carbodiimide method (method II). For the difficult coupling of two successive TOAC residues, the substitution of HOBt with HOAt (1-hydroxy-7-azabenzotriazole)³² gave satisfactory results (method III).

The physical properties of the newly synthesized peptides are listed in Table 1. The synthesis and characterization of pBrBz-TOAC-(L-Ala)₂-TOAC-L-Ala-NHtBu are reported in ref 24.

Typical coupling procedures used were the following:

Method I—Fmoc-Aib-TOAC-(L-Ala)₂-OtBu. To a stirred solution of H-TOAC-(L-Ala)₂-OrBu (0.340 g, 0.82 mmol) in 3 mL of anhydrous CH₂Cl₂, the symmetrical anhydride of Fmoc-Aib-OH (0.570 g, 0.90 mmol) was added, followed, after 30 min, by 0.050 mL (0.045 mmol) of 4-methylmorpholine (NMM). After stirring overnight, the solvent was removed under reduced pressure, the residue was dissolved in AcOEt, and the organic layer was washed with 10% KHSO₄, water, 5% NaHCO₃, and water, dried over Na₂SO₄, then filtered and concentrated under reduced pressure. The peptide was purified by means of flash chromatography on a silica column and eluted with a 98:2 CHCl₃:EtOH mixture. Crystallization from AcOEt/PE afforded the product in 82% yield.

Method II—Fmoc-TOAC-(L-Ala)₃-OtBu. To a suspension of Fmoc-TOAC-OH (1.750 g, 4 mmol) and HOBt (0.578 g, 4 mmol) in 10 mL of CH₂Cl₂ at 0 °C, 1-(3-(dimethylamino)propyl)-3-ethylcarbo-

diimide hydrochloride (EDC·HCl) (0.770 g, 4 mmol) was added. When the suspension had become clear, H-(L-Ala)₃-OrBu (1.150 g, 4 mmol), dissolved in 5 mL of CH₂Cl₂, was added and allowed to stir overnight at room temperature. The solvent was then removed under reduced pressure. The residue was dissolved in AcOEt and the organic layer was washed with 10% KHSO₄, water, 5% NaHCO₃, and water, dried over Na₂SO₄, filtered, and concentrated under reduced pressure. Precipitation with petroleum ether afforded the peptide in a 90% yield.

Method III—Boc-(TOAC)₂-(L-Ala)₄-OrBu. To a suspension of Boc-TOAC-OH (0.035 g, 0.11 mmol) and HOAt (0.015 g, 0.11 mmol) in 1 mL of CH₂Cl₂, at 0 °C, was added EDC·HCl (0.021 g, 0.11 mmol). Then a solution of H-TOAC-(L-Ala)₄OtBu (0.05 g, 0.09 mmol) in 1 mL of CH₂Cl₂ was added. After stirring 4 days at room temperature, the reaction mixture was applied on a flash chromatography silica column and eluted with a 95:5 CHCl₃:EtOH mixture. The peptide was crystallized from AcOEt/PE. Yield: 35%.

Characterization by Electron Spin Resonance. Continuous wave spectra of the peptides were obtained using a Bruker ESP-380 equipped with a TE₁₀₂ cavity. The spectra were independent of concentration in the range studied (0.1 to 1.2 mM). The modulation frequency was 100 kHz, the amplitude was 0.2 G, and the typical scanwidth was 100 G except where otherwise noted. MeOH and EtOH (A.C.S. grade) were obtained from Fischer, 2,2,2-trifluoroethanol (TFE) (NMR grade) came from Aldrich, and 1,1,1,3,3,3-hexafluoroisopropyl alcohol (HFIP) (HPLC grade) was obtained from Sigma.

Results and Discussion

I. 3₁₀-Helix Is the Observed Conformation. Spectra of the hexapeptides in the four alcohols are presented in Figure 2. The line shapes of the spectra are analyzed in terms of the biradical interaction between the two TOAC labels. The strength of the biradical interaction is characterized by the *J*-coupling between electron spins. In the motional-narrowing

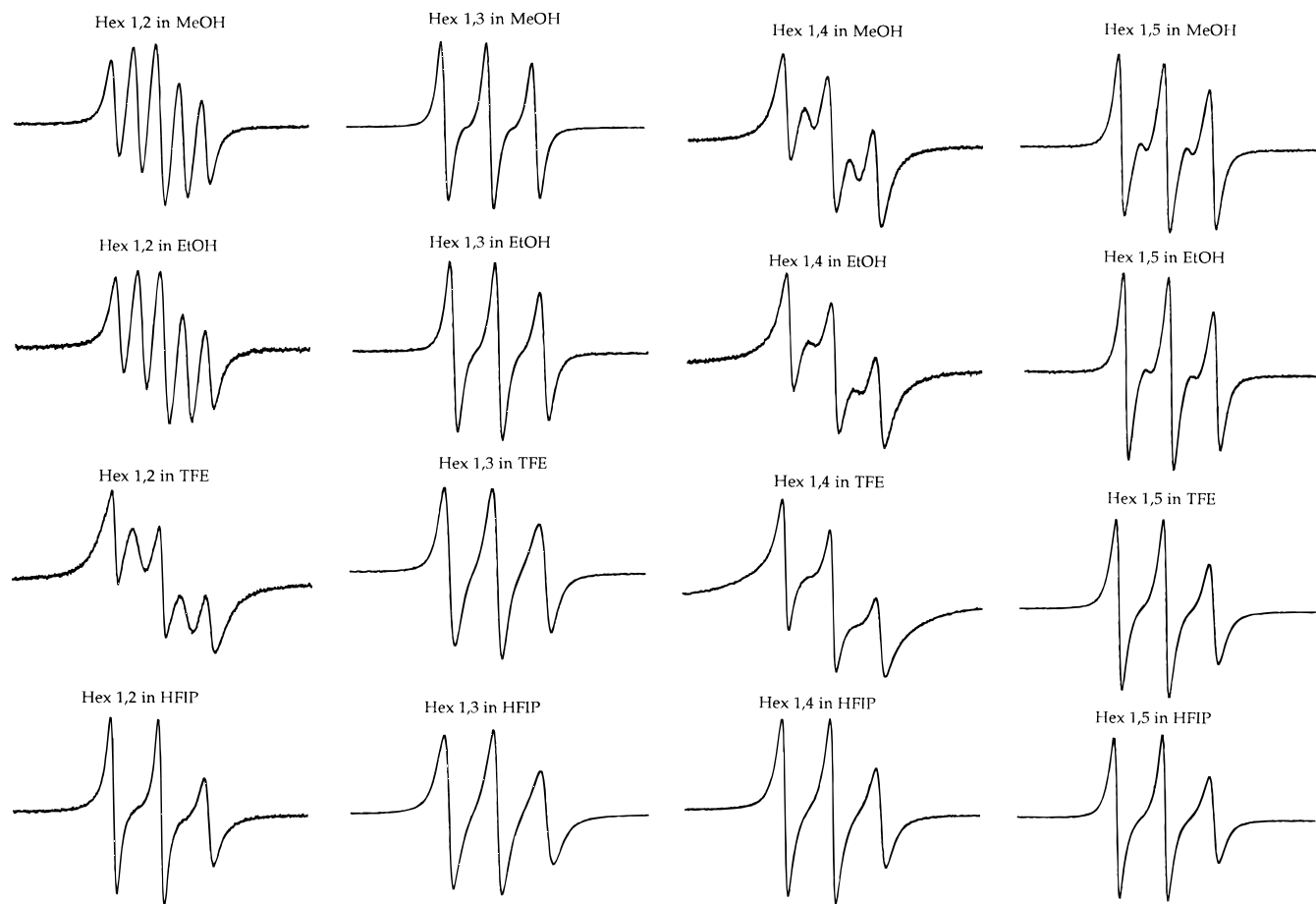


Figure 2. ESR spectra (100 G scanwidth) of the hexapeptides in the four alcohols at 298 K.

regime, the shape of the ESR spectrum is dictated by the degree of J -coupling and isotropic hyperfine coupling, a_n , to the nitroxide nitrogen nucleus. J -coupling increases with decreasing distance (D_{ij}) between labels and, therefore, reports on the relative interlabel distances.²⁻⁴ When J is zero, the ESR spectrum is characterized by three hyperfine lines as found for a monoradical nitroxide species. As J increases, the hyperfine lines broaden and begin to form complex multiplets. When J becomes large relative to a_n (strong exchange) the spectrum is characterized by a five line pattern with an intensity ratio of 1:2:3:2:1 separated by $a_n/2$.

As observed in Figure 2, biradical coupling is clearly indicated in a number of spectra. When analyzing these data, it is recognized that there are two possible helical conformers—the α -helix and 3_{10} -helix—as well as extended nonhelical structure. Molecular models of the peptides, in both the α - and 3_{10} -helical conformations, were built using crystallographically-determined ϕ, ψ values.³³ The resulting through-solvent distances between the nitroxide nitrogens for the doubly-labeled peptides in each conformation are the following:

	$D_{1,2}$	$D_{1,3}$	$D_{1,4}$	$D_{1,5}$
3_{10} -helix	9.75 Å	9.94 Å	6.94 Å	10.82 Å
α -helix	9.54 Å	10.78 Å	7.70 Å	7.96 Å

In all the solvents, save for HFIP which is helix disrupting, the relative strengths of biradical interaction indicate $D_{1,2} < D_{1,4} < D_{1,5} \leq D_{1,3}$. According to the distances above, $D_{1,2}$ should be greater than $D_{1,4}$. Consequently, the strong J -coupling observed for $D_{1,2}$ implies that another biradical mechanism contributes to the strongly J -coupled spectrum observed for *Hex*-

1,2. One possible mechanism for the strong biradical signal is through-bond J -coupling. In contrast to through-solvent J -coupling, through-bond coupling arises from spin-polarization of connecting σ -bonds between labels.³⁴ Spin polarization decreases exponentially with the number of σ -bonds between labels.³⁵ Work with randomly oriented acyl-alkyl biradicals, of seven to twelve carbons in length, has demonstrated such an exponential dependence of this through-bond contribution.³⁶ In *Hex-1,2*, there are nine σ -bonds between the two TOAC nitroxide radicals. Using parameters from Closs et al.,³⁶ the estimated contribution from through-bond coupling in *Hex-1,2* is approximately 230 G. This value is sufficient to give a 1:2:3:2:1 pattern, and it clearly indicates a through-bond contribution to the observed J -coupling in *Hex-1,2*. Nitroxide biradicals may possess even stronger through-bond coupling than acyl-alkyl biradicals due to polypeptide backbone conformational preferences (M. Forbes, personal communication), although further work would be needed to verify this. The five line pattern of *Hex-1,2*, although conformationally sensitive, does not provide direct information for ranking the relative distances between the spin labels.

In the *Hex-1,3*, *-1,4* and *-1,5* spectra in MeOH, the strength of the biradical interaction is greatest in *Hex-1,4* where the five line pattern is clearly observed, although the second and fourth lines are broadened (discussed further below). The biradical interaction is weaker in *Hex-1,5*, where only a hint of a five line pattern is observed, and nearly absent in *Hex-1,3*. The

(34) Luckhurst, G. R. *Biradicals as Spin Probes*; Academic Press: New York, 1976, pp 133-181.

(35) Onuchic, J. N.; Beratan, D. N. *J. Am. Chem. Soc.* **1987**, *109*, 6771-6778.

(36) Closs, G. L.; Forbes, M. D. E.; Piotrowiak, P. *J. Am. Chem. Soc.* **1992**, *114*, 3285-3294.

(33) Toniolo, C.; Benedetti, E. *Trends Biochem. Sci.* **1991**, *16*, 350-353.

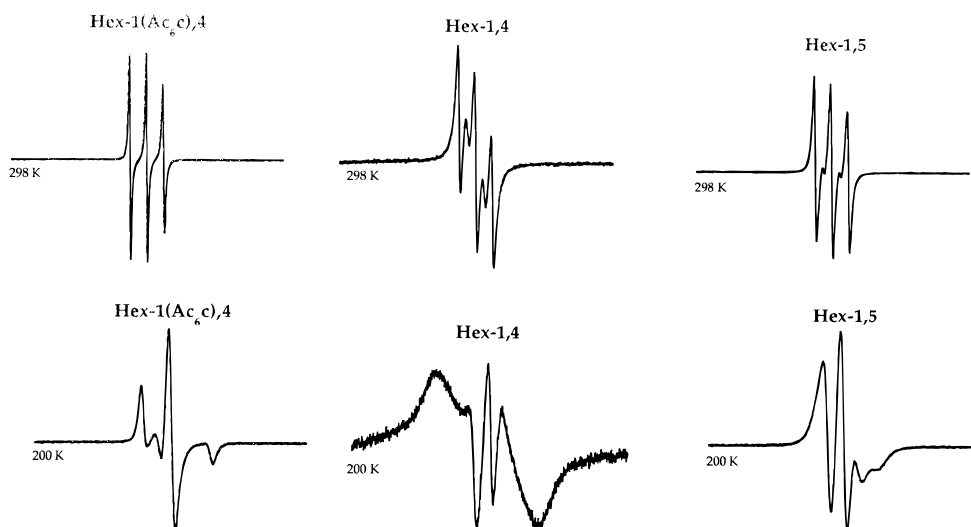


Figure 3. Spectra (250 G scanwidth) of the singly and doubly labeled hexapeptides at 298 and 200 K in MeOH.

observation of little biradical interaction for *Hex-1,3* indicates that the through-bond contribution is too weak to influence the spectral shape of an $i \rightarrow i + 2$ doubly labeled peptide. The J -coupling hierarchy indicates $D_{Hex-1,4} < D_{Hex-1,5} < D_{Hex-1,3}$. The distances reported above indicate that the 3_{10} -helical conformation follows $D_{1,4} \ll D_{1,5}$ whereas the α -helical conformation follows $D_{1,4} \approx D_{1,5}$. Therefore, the hierarchy of biradical interactions suggests that the hexamers in MeOH are in a 3_{10} -helical conformation. This is consistent with crystallographic work on peptides containing Aib. Short peptides ($n < 8$) with two or more Aib residues always crystallize as 3_{10} -helices.^{10,11} Furthermore, we have shown in a crystallographic study that a $i, i + 3$ doubly TOAC labeled pentapeptide adopts a 3_{10} -helical conformation.²⁴ The spectrum of this pentapeptide is nearly superimposable on that of *Hex-1,4* which further suggests that the two peptides adopt the same structure in solution.

In addition to J -coupling, biradicals also exhibit electron–electron dipolar coupling. The strength of this interaction is determined by $1/D_{ij}^3$.³⁴ For rapidly tumbling peptides, the dipole–dipole tensor averages to zero and does not contribute to the ESR spectrum. However, for slowly tumbling or immobile systems, the strength of the dipolar interaction serves as a measure of the distance between the coupled spins. To test the assignment of 3_{10} -helix as the dominant conformer, we examined *Hex-1,4* and *Hex-1,5* in MeOH at a reduced temperature of 200 K. As a control for peptide mobility, we also examined the singly spin labeled peptide *Hex-1(Ac6c)4*. The results are shown in Figure 3. At low temperature, the peptide rotational correlation time increases and 200 K was found to be the highest temperature at which *Hex-1(Ac6c)4* gave the expected spectrum for an immobile nitroxide. *Hex-1,4* shows the broad pattern expected for a biradical exhibiting strong dipolar coupling. However, *Hex-1,5* shows only slight broadening as compared to the monoradical. These spectra are in stark contrast to spectra recently reported for doubly TOAC labeled α -helical peptides in which the dipolar interaction was much larger for the $i, i + 4$ analog.²⁵ These findings provide strong support for the assignment of 3_{10} -helix as the dominant conformer of the hexapeptides.

II. Solvent Influences Helical Structure. Figure 2 demonstrates that solvent plays an important role in determining helical structure. Comparison of the hexapeptide spectra in MeOH with the spectra in EtOH indicates that the biradical character of both *Hex-1,4* and *Hex-1,5* is diminished. The second and fourth hyperfine lines are broadened and appear less

intense. In contrast, the spectra of *Hex-1,2* and *Hex-1,3* are relatively unchanged except for a small amount of additional line broadening for *Hex-1,3*. As discussed, the J -coupling observed for *Hex-1,2* reflects both a through-bond and through-solvent interaction. Through-bond coupling is governed by the intervening dihedral angles and is therefore very sensitive to local conformation. That the *Hex 1,2* spectra are similar in MeOH and EtOH suggests that the TOAC-TOAC dipeptide unit retains the helical conformation. However, the decrease of biradical signal for *Hex-1,4* and *Hex-1,5* indicates that there is partial disruption of the full helical turn. In addition, selective broadening of the second and fourth lines is characteristic of flexible biradicals³⁷ and that the peptides are “flickering” in and out of the helical conformation. Such an observation is consistent with the concept of the nascent helix from NMR spectroscopy where, in an ensemble of peptide conformations, sequential NOE’s indicate a substantial population of the helical region in ϕ, ψ space, but with insufficient overall helical structure to yield medium-range helical NOE’s.³⁸ Thus, for partially folded peptides, short-range order is approximately maintained but regular helical structure is disrupted and accompanied by an increase in the local dynamics.

In TFE, the second and fourth lines of the *Hex-1,2*, *Hex-1,4*, and *Hex-1,5* spectra have broadened substantially relative to the spectra in non-fluorinated MeOH and EtOH. In fact, for *Hex-1,5* the second and fourth hyperfine lines are no longer detectable. The *Hex-1,5* spectrum is typical of a weakly interacting biradical ($J \ll a_n$) which is characterized by a three-line hyperfine pattern broadened by the biradical interaction. (The three nitroxide hyperfine lines are broader than a simple monoradical nitroxide due to a superposition of singlet and nearby triplet transitions. The line widths of the three observed hyperfine lines increase with the degree of J -coupling.³⁴) *Hex-1,4* shows more biradical coupling than *Hex-1,5* and still exhibits a hint of strong coupling. These data suggest that TFE is less helix promoting than MeOH or EtOH.

Spectra for the hexamers in HFIP reveal little biradical interaction. The peptides give spectra in HFIP that are nearly superimposable and similar to monoradical spectra. Thus, in HFIP there is no detectable helical population.

Neat TFE and HFIP are more polar than either MeOH or EtOH. Recent ESR studies suggest that less polar solvents enhance peptide helix content.²⁴ Sankarapandi *et al.* examined

(37) Luckhurst, G. R.; Pedulli, G. F. *Mol. Phys.* **1971**, *20*, 1043–1055.

(38) Dyson, H. J.; Rance, M.; Houghten, R. A.; Wright, P. E.; Lerner, R. A. *J. Mol. Biol.* **1988**, *201*, 201–217.

a peptide designed to mimic a type II β -turn and showed that solvents of varying polarity have a dramatic influence on turn structure.³⁹ The effects of solvent polarity have also been observed in an X-ray diffraction study by Karle *et al.*¹³ in which the structure of Boc-Val-Ala-Leu-Aib-Val-Ala-Leu-OMe revealed an increase of helix fraying with increasing polarity of the crystallization cosolvent. Fraying seems to result from the insertion of cosolvent molecules into the peptide backbone C=O \cdots H-N ($i \leftarrow i + 3$ or $i \leftarrow i + 4$) hydrogen bonds. However, helical contacts are still present indicating preference for the helical conformation.

Brooks and Nilsson used molecular dynamics to calculate the detailed free energy surfaces of a blocked Ala tripeptide in the neat solvents MeOH, TFE, and water and in mixtures of water/MeOH and water/TFE.⁴⁰ Distinct free energy minima were found for the helix and extended strand conformations. They predicted that neat MeOH would stabilize helix relative to extended strand ($\Delta A \approx 1.0$ kcal/mol) and, in contrast, that neat TFE would destabilize helix ($\Delta A \approx -2.1$ kcal/mol). The experiments reported here strongly support these predictions. However, it should be noted that the ESR experiments shown in Figure 2 suggest that, in the longer hexameric peptides studied here, neat TFE does not lead to complete unfolding of the helical structure.

ESR spectra can provide insight into the time scale of peptide dynamics. Conformational flickering leads to time-dependent modulation of the J -coupling. For example, consider the *Hex-1,4*. In MeOH, there is a distinct five line pattern indicating strong J -coupling consistent with the helical conformation; however, the second and fourth hyperfine lines are weaker than the remaining lines. When the peptide is unfolded in HFIP the J -coupling is barely detectable. The most noticeable difference between the two spectra is the presence of the second and fourth hyperfine lines. The shapes of these two hyperfine lines are very sensitive to time-dependent modulation of the J -coupling.^{41,42} There are two motional regimes to consider: fast interconversion and slow interconversion. The reference point distinguishing the two cases is the isotropic hyperfine constant a_n . Taking τ as the mean lifetime for the helical conformation, $\tau a_n \gg 1$ is slow interconversion. ESR spectra in this regime are composed of a superposition of a strongly J -coupled spectrum from helix and an uncoupled spectrum from an extended strand. The population of the strongly coupled spectrum determines the strength of the second and fourth transitions. When $\tau a_n \ll 1$, the interconversion is fast and the spectrum is determined by the population-weighted average J from helix and extended strand. If this average J is still much greater than a_n , the spectrum will be characterized by a 1:2:3:2:1 five line pattern. However, if the product τa_n approaches unity, the second and fourth transitions broaden due to rapid spin-spin relaxation. Thus, weak second and fourth transitions can arise from either fast or slow interconversion. The best way to distinguish the two cases is with variable temperature experiments. Decreasing the temperature for the *Hex-1,4* in MeOH leads to further broadening of the second and fourth transitions (data not shown) just as has been found in a previous study of the *pBrBz-Pent-1,4*.²⁴ Decreasing the temperature should slow the interconversion rate (and increase τ). Concomitant increase in τ and increase in the linewidths of the second and fourth transitions indicates that interconversion

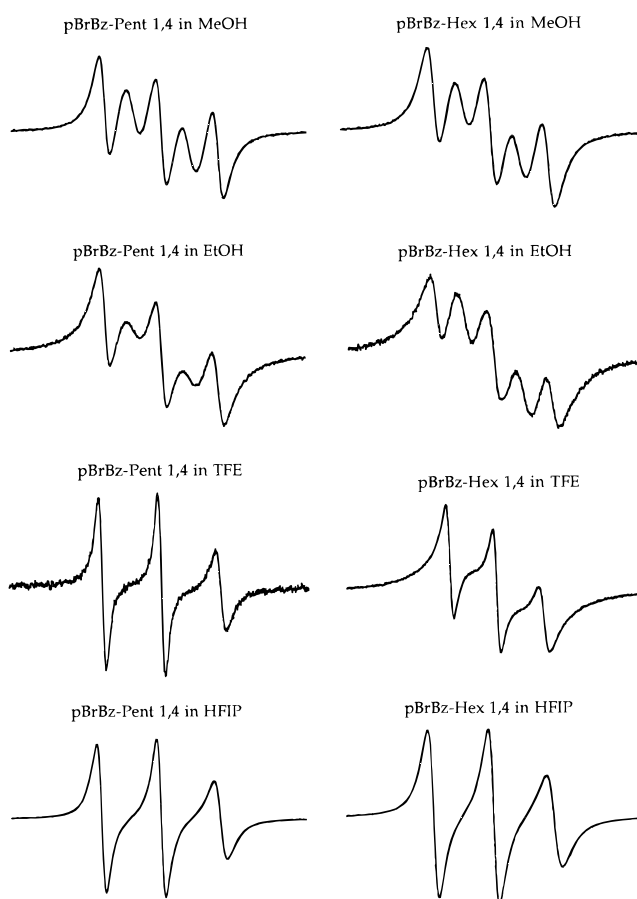


Figure 4. ESR spectra of the penta- and hexapeptides N $^{\alpha}$ -blocked with the *pBrz* group in the four alcohols at 298 K.

between helix and extended structure is fast. Thus, $\tau \leq a_n^{-1} \approx 3.5 \times 10^{-9}$ sec and this constraint places an upper bound on the helix lifetime. It appears that helix/coil interconversion takes place on the nanosecond time scale. Our results suggest that a well-structured turn of helix, as indicated by $i \rightarrow +3$ J -coupling, has a lifetime of between 1 and 3 ns.

Our estimates of the helix/coil interconversion kinetics compare well with molecular dynamic calculations. Simulations suggest that hydrogen bonds in helical peptides break and reform within 0.5 to 1 ns (recently reviewed by Brooks and Case⁴³). Just recently, Brooks used master equation calculations to examine helix folding kinetics for peptides of various lengths.⁴⁴ Both folding and unfolding for short peptides took place in less than 5 ns—a value that agrees well with the experimental findings presented here. From a different experimental perspective, Williams *et al.*⁴⁵ have used temperature jump techniques to probe the folding kinetics of a 21-residue Ala-rich peptide. They found that helix folding took place with a half-life of approximately 16 ns. Given that longer peptides should exhibit slower interconversion kinetics, our results appear to be in reasonable agreement with those of Williams *et al.*

III. Helical Structure Is Influenced by the N $^{\alpha}$ -Blocking Group, Main-Chain Length, and Aib Content. The peptides in Figure 2 are blocked at the N-terminus with the Boc carbamate moiety. In Figure 4 are shown spectra of similar peptides blocked with a *para*-bromobenzoyl (*pBrBz*) amide group. Comparison of the spectra from *pBrBz-Hex-1,4* and

(39) Sankarapandi, S.; Sukumar, M.; Balaram, P.; Manoharan, P. T. *Biochem. Biophys. Res. Commun.* **1995**, *213*, 439–446.

(40) Brooks, C. L.; Nilsson, L. *J. Am. Chem. Soc.* **1993**, *115*, 11034–11035.

(41) Luckhurst, G. R. *Mol. Phys.* **1966**, *10*, 543–550.

(42) Parmon, V. N.; Zhidomirov, G. M. *Mol. Phys.* **1974**, *27*, 367–375.

(43) Brooks, C.; Case, D. *Chem. Rev.* **1993**, *93*, 2487–2502.

(44) Brooks, C. L. *J. Phys. Chem.* **1996**, *100*, 2546–2549.

(45) Williams, S.; Causgrove, T. P.; Gilmanshin, R.; Fang, K. S.; Callender, R. H.; Woodruff, W. H.; Dyer, R. B. *Biochemistry* **1996**, *35*, 691–697.

Hex-1,4 (Figure 2) reveals a stronger biradical interaction for the *pBrBz* blocked peptide in MeOH and EtOH. An amide carbonyl exhibits similar basicity to a carbamate carbonyl so the two blocking groups are expected to exhibit similar hydrogen bond strengths.^{46,47} However, the *pBrBz* possesses an aromatic π -structure that extends through the N-terminal amide bond. Thus, *pBrBz* is rigidly attached and coplanar with this N-terminal amino group. The crystal structure of a doubly TOAC labeled pentapeptide²⁴ has demonstrated this coplanarity and indicates that there are no unfavorable steric contacts for the *pBrBz* blocking group. In contrast, the Boc group⁴⁸ can undergo rotation about the O–C bond where the group attaches to the first amide carbonyl. Molecular models built for a helical hexapeptide suggest that steric interactions limit the rotameric states available to the Boc group. This suggests that there is a loss of conformational entropy for the Boc group upon helix formation which slightly shifts the equilibrium to random coil. Doig et al.⁴⁹ have recognized that acetyl (Ac) is a better N-terminal capping group than 18 of the 20 natural amino acids even when N-terminal charge is eliminated. The physical basis for the enhanced helix stability conferred by Ac remains unclear. *pBrBz* and Ac are similar in that both are rigidly attached to the N-terminal amino group. However, an unblocked amino acid contributes only its amide carbonyl to the first helix hydrogen bond. Consequently, the N-terminal unblocked amino acid is conformationally flexible even more than the Boc protecting group. If this conformational freedom is lost upon helix formation, the analysis presented here suggests that the associated loss of entropy would increase the free energy of the folded state.

The difference in stability upon going from Boc to *pBrBz* appears to be substantial. The *pBrBz* blocked peptide exhibits greater biradical coupling in MeOH. Furthermore, in EtOH, *pBrBz-Hex-1,4* exhibits greater biradical coupling than *Hex-1,4* in MeOH. Thus, the tendency of EtOH to partially unfold a hexameric sequence is more than offset by the *pBrBz* blocking group. The solvent-induced unfolding pattern is also different as a function of the different N $^{\alpha}$ -blocking groups. Whereas for Boc the unfolding is gradual, with each solvent of increased polarity giving slightly weaker biradical coupling, the change for *pBrBz* is sudden, with EtOH giving a well-structured helix and TFE giving a much weaker biradical spectrum. The origin of this change may be the highly helical nature of *pBrBz-Hex-1,4* which undergoes a more cooperative unfolding transition as solvent polarity is increased. It should be noted that Doig et al.⁴⁹ have recently demonstrated the substantial influence of N $^{\alpha}$ -blocking groups on water-soluble helical peptides and they also modified Lifson–Roig helix–coil theory to include the added stability.

In Figure 4, the spectra of *pBrBz-Pent-1,4* and *pBrBz-Hex-1,4* are compared. The two peptides differ in length by one Ala residue. However, because of the different C-terminal blocking groups, both peptides contain the same number of backbone amide groups. Comparison of the spectra in MeOH reveals nearly identical biradical spectra, *i.e.* both peptides are highly helical. In EtOH *pBrBz-Pent-1,4* exhibits an observable reduction in the biradical interaction which indicates a partial loss of structure. In contrast, *pBrBz-Hex-1,4* in EtOH maintains a five line pattern similar to that of the MeOH data. The

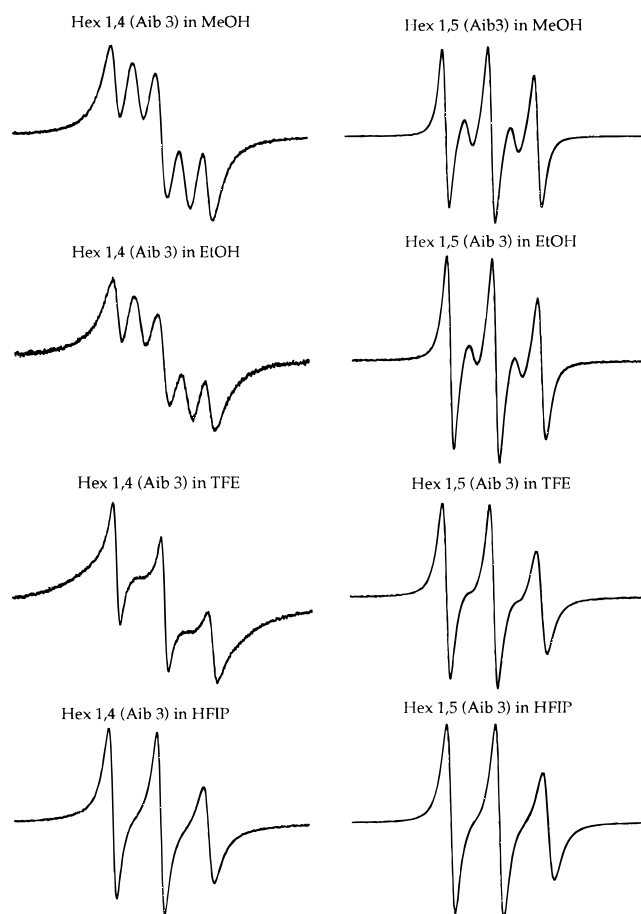


Figure 5. ESR spectra of the hexapeptides containing an Aib at position 3 in the four alcohols at 298 K.

additional amino acid exerts a stabilizing influence upon the structure due to the increase in sequence length. The observed increase in helix stability with increasing main-chain length is consistent with previous observations.^{4,14,50} However, detection of increased stability from a single Ala is striking. (Interestingly, the addition of an Ala to the sequence is not nearly so effective at stabilizing these peptides as controlling the N $^{\alpha}$ -blocking group.)

Figure 5 shows the spectra of hexapeptides containing an Aib guest between the label positions (position 3, see Figure 1 for sequences). The degree of *J*-coupling for both of the modified peptides is noticeably greater than in the corresponding parent peptides. In fact, the biradical interaction for *Hex-1,4 (Aib 3)* in MeOH is the strongest of all the *1,4* peptides in this study. In contrast to observations made for the parent peptides in the same solvent systems, the spectra of the guest peptides differ very little as the solvent is changed from MeOH to EtOH. This indicates that, similar to the *pBrBz* N $^{\alpha}$ -blocking group, Aib confers sufficient helix stabilization to more than offset the difference between the two solvents. Unlike the *pBrBz* blocked peptides, the *Hex-1,4 (Aib 3)* peptide does not completely unfold in TFE. Thus, inclusion of an Aib in the sequence increases both helix content and the resistance to unfold in polar solvents. The solvent-induced unfolding also appears to be less cooperative than that found for the helix-stabilizing N $^{\alpha}$ -blocking group. Nevertheless, the final set of spectra indicate that HFIP is able to unfold these Aib-containing sequences.

These results reinforce the helix-stabilizing role played by C $^{\alpha}$ -tetrasubstituted amino acids (such as Aib and TOAC). For

(46) Parmentier, J.; Samyn, C.; Van Beylen, M.; Zeegers-Huyskens, T. *J. Chem. Soc., Perkin Trans. 2* **1991**, 387–392.

(47) Vanswevelt, H.; Vanquickenborne, L.; Van der Vorst, W.; Parmentier, J.; Zeegers-Huyskens, T. *Chem. Phys.* **1994**, *182*, 19–26.

(48) Benedetti, E.; Pedone, C.; Toniolo, C.; Nemethy, G.; Pottle, M. S.; Scheraga, H. A. *Int. J. Pept. Protein Res.* **1980**, *16*, 157–172.

(49) Doig, A. J.; Chakrabarty, A.; Klingler, T. M.; Baldwin, R. L. *Biochemistry* **1994**, *33*, 3396–3403.

(50) Pavone, V.; Benedetti, E.; Di Blasio, B.; Pedone, C.; Santini, A.; Bavoso, A.; Toniolo, C.; Crisma, M.; Sartore, L. *J. Biomol. Struct. Dyn.* **1990**, *7*, 1321–1331.

example, stabilization of helices with Aib has been clearly demonstrated crystallographically in short 6–9 residue peptides where insertion of a single Aib is sufficient to initiate helix formation.^{10,11} Similar trends have also been observed for a limited number of Aib-rich peptides in organic solvents^{17–20} and molecular dynamics have shown that a single Aib incorporated into a poly(Ala)_n peptide increases the helical content of the peptide.⁵¹ As has been well-established, the conformation of C^α-tetrasubstituted amino acids tends to favor the helical region of ϕ, ψ space.^{9–11} *Hex-1,4* (Aib 3) and *Hex-1,5* (Aib 3) contain three C^α-tetrasubstituted amino acids and exhibit enhanced stabilization over *Hex-1,4* and *Hex-1,5* which contain only the two TOACs. However, even with three C^α-tetrasubstituted amino acids, there is no detectable helical structure in HFIP. While TOAC (and Aib) are clearly helix favoring, they do not lock a peptide into a helical conformation.

The data presented above demonstrate the presence of helix in the hexameric sequences. However, the actual helix content under folding conditions has not yet been addressed. Do conditions favoring helix yield a uniformly folded structure? Circular dichroism is a standard benchmark for determining peptide helicity. However, TOAC exhibits a UV absorbance that, when attached to a helical peptide, contributes to the CD signal. Thus, CD does not provide a reliable measure for determining helix content in these short peptides. It is also difficult to determine helix content directly from the motionally-narrowed ESR biradical spectra. Biradical spectra dominated by *J*-coupling are clearly useful for ranking distances but spectral line shapes alone cannot yield quantitative distances, especially in the strong coupling regime. Thus, the distance constraints useful for determining helical content are not available. However, we can offer the following argument. Figure 5 shows a strong biradical signal for *Hex-1,4* (Aib 3) and partial biradical signal for *Hex-1,5* (Aib 3) in EtOH. As noted, the observed biradical interactions are greater for these Aib-containing peptides in EtOH than for the parent peptides (without Aib) in MeOH. When the Aib-containing peptides are placed in MeOH, there is almost no increase in the observed biradical interaction. It appears that there is no further increase in helix structure even with the use of the more helix-favoring solvent. We propose that the *Hex-1,4* (Aib 3) and *Hex-1,5* (Aib 3) peptides are completely folded in MeOH and EtOH and that the spectra of these peptides provide benchmarks for the helical state. Likewise, the absence of helical biradical interactions observed for any of the peptides in HFIP indicates that there is little helical structure in this solvent. The remaining sequence/solvent combinations yield partially folded structures. Further work will

be required before the helix content can be estimated for these partially folded cases.

Since TOAC stabilizes helix structure and is not simply a benign conformational reporter, there is concern as to whether the relative placement of the TOAC's influences helical content. For instance, does *Hex-1,2* have the same structure as *Hex-1,5*? The sequences studied here do not directly address this issue. However, Karle and Balam¹⁰ have examined the conformational trends of Aib-rich peptides and they find that the α -helix \leftrightarrow 3_{10} -helix equilibrium is controlled mainly by Aib content and not the relative placement of helix-forming residues. As noted by both Karle¹⁵ and Bindra et al.,¹⁸ percent Aib content and peptide length are the major factors that control peptide conformation. Nevertheless, these authors have demonstrated that, under certain conditions, an α -helix \rightarrow 3_{10} -helix transition can occur upon sequence permutation. Whether the conformational equilibrium among 3_{10} -helix and α -helix is influenced by sequence permutation for short peptides remains an open question to be addressed in future work.

Conclusion

The findings presented here demonstrate that ESR of doubly TOAC labeled peptides is a useful technique for probing the factors that control helix structure. One may explore Ala-rich peptides containing C^α-tetrasubstituted residues without the concern of signal overlap that often hampers NMR investigations. For rapidly tumbling peptides, such as the hexamers, *J*-coupling and helix dynamics determine the shape of the biradical spectra. Solvent, sequence length, N^α-terminal blocking group and C^α-tetrasubstituted residues all influence the structure of the hexameric sequences. Even though crystallographic studies have demonstrated the importance of these factors in helix stabilization, the experiments here represent a systematic approach for solution studies. Furthermore, solution studies using ESR are sensitive to the time scale for helix \rightarrow coil interconversion. While it is reassuring that crystallography and solution magnetic resonance are in agreement with regards to the factors that stabilize peptide helices, it is also clear that important new information is available from solution studies of spin-labeled peptides.

Acknowledgment. The authors are grateful to Gary Martinez for help with interpretation of the dipolar spectra and to Dr. Kim Bolin for many helpful comments on the manuscript. This work was supported by an NIH grant (GM 46870) and a grant from the University of California Systemwide Biotechnology Program.

(51) Zhang, L.; Hermans, J. *J. Am. Chem. Soc.* **1994**, *116*, 11915–11921.